Earth Surface Processes and Landforms
Earth Surf. Process. Landforms **30**, 121–127 (2005)
Published online in Wiley InterScience (www.interscience.wiley.com). **DOI:** 10.1002/esp.1140

Technical Communication

Texture-based image segmentation applied to the quantification of superficial sand in salmonid river gravels

Patrice E. Carbonneau[1]*, Normand E. Bergeron[1] and Stuart N. Lane[2]
[1] *Institut National de la Recherche Scientifique, Centre eau, terre et environement, Québec, Canada*
[2] *Department of Geography, University of Durham, Durham, UK*

**Correspondence to:*
P. E. Carbonneau, 490 rue de la Couronne, Québec, G1K 9A9, Canada. E-mail: patrice_carbonneau@inrs-ete.uquebec.ca

Received 16 May 2003;
Revised 5 April 2004;
Accepted 21 May 2004

Abstract

The presence of fine sediment in river gravels is widely recognized as being detrimental to salmonid habitat quality. In order to facilitate quantification of sand presence at larger scales, this paper presents an application of image processing allowing for rapid and accurate assessments of superficial sand presence in dry exposed fluvial gravels. Images for the process are acquired with a 35 mm SLR film camera and then scanned with a desktop scanner. Texture-based segmentation is then applied to differentiate between sand and clast areas. Results show that the method is accurate and therefore it offers an alternative to bulk sampling in cases where rapid assessments of sand presence are required. Copyright © 2005 John Wiley & Sons, Ltd.

Keywords: image processing; image texture; gravel-bed rivers; sand deposition

Introduction

The detrimental effects of fine sediment in fluvial gravels on salmonid habitat quality are well documented (Hall and Baker, 1982; Chapman, 1988). During the incubation phase, it has been shown that the presence of fine sediment within the gravel matrix reduces the survival rate of the eggs (Sear, 1993; Wu, 2000; Soulsby *et al*., 2001). Furthermore, Cunjak *et al*. (1998) suggested that during the juvenile life stage, sand deposition on the surface of the bed could block access to the large interstitial voidspaces used by juvenile salmon as shelter during overwintering. The assessment of habitat quality in gravel-bed rivers must therefore take into account the presence of sand. Furthermore, the presence of surface sand is an important factor in defining and identifying major surface structure types (Church *et al*., 1987; Bunte and Abt, 2001). Embeddedness is recognized as being a bed structure with potential detrimental impacts on salmonid habitat quality (Bunte and Abt, 2001). It is defined as the partial burial of coarse clasts by fine sediment. The methods developed to quantify embeddedness (e.g. Bunte and Abt, 2001) all rely on measurements of the coarse clast position relative to the bed and do not explicitly use quantification of sand presence in the quantification of embeddedness. However, an objective procedure which quantifies surface sand presence in areal units would provide useful data towards the quantification of embeddedness. However, all the existing methods applicable to the quantification of sand presence are volumetric. In procedures such as bulk sampling, all bed material must be excavated and then measured by weight or volume. In such procedures, the *position* of the sand relative to coarse particles is lost. Therefore, there currently is a methodological void pertaining to areal quantification of surface sand presence in river gravels. Whilst time-consuming manual measurement of the surface of sandy patches in the field would be possible, a faster method based on terrestrial remote sensing should be achievable.

The objective of this paper is to develop such a method based on image processing and capable of rapid and accurate assessments of superficial sand presence in gravel environments. Texture-based image segmentation was applied to close-range imagery of the bed in order to achieve a reliable and fully automated procedure capable of quantifying the extent of sand patches in images.

Image Segmentation Theory Applied to Sand Identification

Automated quantification of sand coverage from imagery can be accomplished through image segmentation. In this case, a given river bed image must be segmented into two classes: coarse clasts (gravels, cobbles, boulders) and finer particles. Once this task is accomplished, the resulting binary image can be used to calculate the percentage of sand coverage in the initial image.

The most common segmentation procedures rely on grey-level histogram segmentation. The assumption in this case is that clasts and sand will belong to two distinct classes in the brightness-level histogram which implies that each clast can be distinguished based on its brightness level. Figure 1 shows an example of grey-level segmentation applied to an image of sand and clasts. Figure 1A shows a raw image with three clasts. One of these clasts is very light in colour and will predictably be easy to detect. The other two have caked sand on their surface and are roughly the same colour as the neighbouring sand. They will be difficult to detect. Figure 1B shows the associated brightness-level histogram. Whilst the histogram does have two peaks which may be associated with sand and clast areas, the peaks are not clearly separated. Application of Otsu's automated thresholding method (Otsu, 1979) to Figure 1A yields a value of 203. If the image in Figure 1A is segmented with a threshold value of 203, Figure 1C is obtained. In Figure 1C white areas (1) correspond to brightness levels below 203 and black areas (0) correspond to areas with brightness greater than or equal to 203. Whilst the result does correctly identify the main clast, the secondary clasts are poorly outlined. Furthermore, several sand particles have brightness levels similar to that of the clasts, which violates

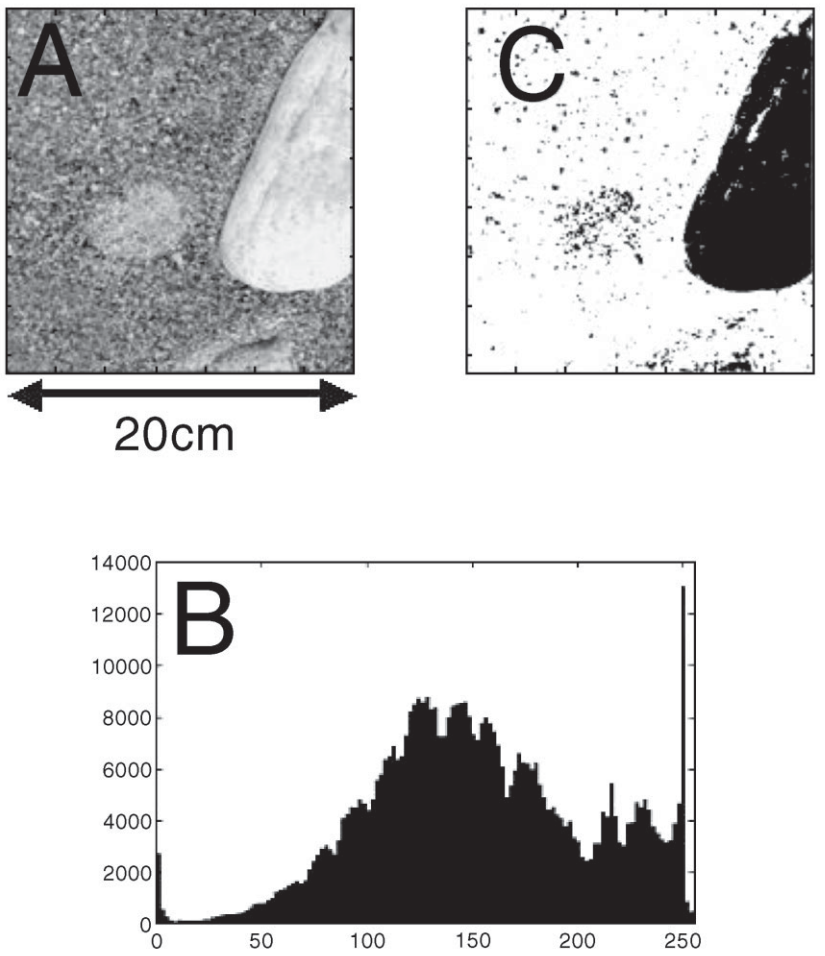

Figure 1. (A) Raw image with sand and clasts. (B) Associated grey-level histogram. (C) Binary classified image with sand in white and clasts in black.

the assumption that sand and clasts are in two distinct brightness classes. This will lead to a false identification of sand particles as very small clasts. This false identification will introduce a background noise in sand coverage estimates.

Figure 1 illustrates the limitations of standard grey-level segmentation when applied to sand/clast imagery. The assumption that sand and clasts are in two different classes is clearly false. Therefore, segmenting clasts and sand solely on the basis of grey levels will predictably give poor results such as seen in Figure 1. In such cases, the segmentation process must detect local grey-level variability caused by the mixture of light and dark sand particles. The study of image texture was developed specifically for the purpose of quantifying spatial patterns and variability in images (Haralick *et al*., 1973). These textural approaches to image segmentation were found to give better results than standard grey-level segmentaion in highly complex imagery (Conners *et al*., 1984; Haralick and Shapiro, 1985) which justifies their application to river gravel imagery.

The accepted definition of image texture is: 'an attribute representing the spatial arrangement of the grey levels of the pixels in a region' (IEEE, 1990). Texture-based segmentation operates by transforming a raw image into a textural measure image where local texture information is represented as grey levels. Image texture is evaluated with the co-occurrence matrix. The co-occurrence matrix is constructed by comparing all image pixels separated by a distance D at direction V. The i, jth element of the co-occurrence matrix $\mathbf{P}$ for an image is the number of times that grey levels i and j occur in two pixels separated by distance D and direction V divided by the total number of pixel pairs (Castleman, 1996). The co-occurrence matrix therefore is of size (G,G) where G is the number of grey levels in the image, usually 256. To make the co-occurrence matrix faster to calculate, the number of grey levels is generally resampled to 8, 16 or 32. Therefore, co-occurrence can quantify how many pixels of similar grey levels are neighbours. Once the co-occurrence matrix is calculated, textural features may be derived to reduce the information in the co-occurrence matrix to a single value (Harralick *et al*., 1973; Conners *et al*., 1984; Castleman, 1996). For example, entropy is defined as:

$$E = \sum_i \sum_j \mathbf{P}_{ij} \log \mathbf{P}_{ij} \tag{1}$$

where E is entropy and $\mathbf{P}$ is the co-occurrence matrix. Areas of high entropy have low texture and are mapped to light grey levels.

If the co-occurrence matrix is calculated for the whole image and then Equation 1 is applied, the texture information for the whole image is reduced to a single number. This removes all spatial information within the image. Therefore, a windowing approach must be used to produce a textural image which retains local image texture properties. To produce the textural image, the co-occurrence matrix is calculated for a window of size (W,W) initially located at the Cartesian origin of the raw (M,N) image. Equation 1 is then used to calculate textural entropy for this window. This entropy value becomes the first pixel in the texture image. The window is then repeatedly translated by one pixel and the process is repeated until the whole image has been covered. The resulting textural image therefore has dimensions $(M - W, N - W)$. Therefore in the texture image, the i, jth pixel is the textural measure value for the co-occurrence matrix of the region $[i: i + W - 1; j: j + W - 1]$ in the original image. The pixel values in the texture image can then be rescaled to 8-bit values (0–255) to make it compatible with standard image processing algorithms. Basic grey-level thresholding methods can then be applied to segment objects in the texture image.

For example, Figure 2A shows the texture image calculated for the image in Figure 1A, and Figure 2B shows the associated histogram. If Figures 1B and 2B are compared, it can be seen that the low intensity peak has been shifted towards the left and its standard deviation is also reduced. This will minimize confusion between classes. If Otsu's method is applied to the image in Figure 2A, the resulting value is 141. The binary image produced from this threshold is shown in Figure 2C. In Figure 2C, the primary clast is still clearly defined. Identification of the secondary clasts has improved slightly and more importantly, light coloured sand particles falsely classified as clasts have been almost completely eliminated. This elimination of noise in the sand detection process is due to the fact that the texture image takes into account the brightness values within a sampling window. Therefore, isolated sand particles which are brighter than their surroundings will not be falsely detected as clasts.

Methods

Imagery

The raw image data for this work was initially collected as part of a close-range photogrammetry survey designed to study the voidspaces in river gravels on the Sainte-Marguerite River, Quebec, Canada. Twenty study sites were

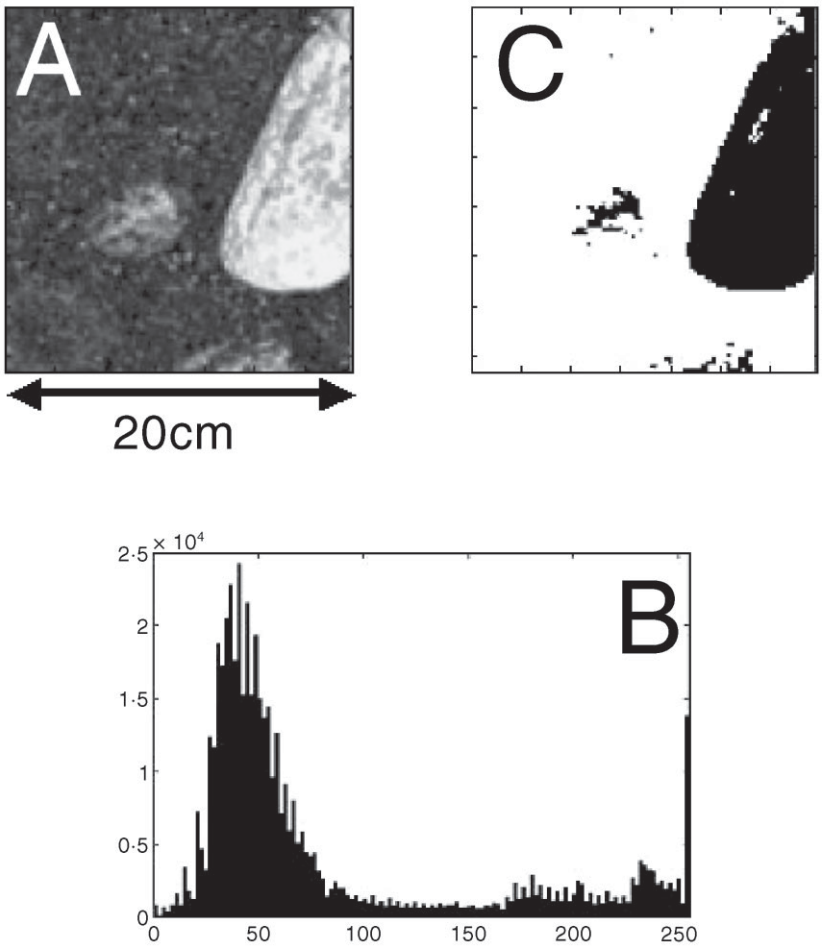

Figure 2. (A) Texture image calculated from Figure 1A. (B) Associated grey-level histogram. (C) Binary classified image with sand in white and clasts in black.

selected to represent a wide range of gravel sizes. Within the 20 sites, six had patches of coarse sand (*c.* 1–2 mm). Images were taken with a commercial 35 mm SLR film camera. The camera was vertically mounted on a gantry with the lens at an elevation of 1·2 m above the bed. Initial images covered 60×40 cm in real space. For the sand quantification work, image prints were scanned in 8-bit (0–255) grey scale with a commercial desktop scanner at 300 dpi. This yielded images of 1800×1200 pixels which equates to a pixel size of similar scale to the size of a medium sand particles (0·3 mm) according to the Wentworth scale (Wentworth, 1922). The central area of each image was then subdivided into four sub-images covering 20×20 cm. Since 14 of 20 sites had no superficial sand, there was an excess of sand-free sub-images. Therefore, 25 sub-images were selected to cover the widest possible range of sand coverage which was found to range from 0 to 84 per cent.

Quantification of Sand Coverage

Textural entropy images were calculated following a windowed application of the co-occurrence matrix and Equation 1 for each of the 25 sub-images. To calculate co-occurrence, images were resampled to 16 grey levels (4 bits). A 20×20 pixel window size was used. The texture images were then automatically segmented into two classes representing sand and clasts with Otsu's method. Furthermore, it was decided that clasts smaller than nine pixels (3×3 mm) should be considered in the sand percentage since these objects are likely associated with the few remaining falsely identified clasts. Each one of these objects was automatically detected are reclassified as sand.

In addition to texture-based segmentation, conventional grey-level segmentation, where Otsu's method is applied directly to the raw image, was applied to image data to allow for a formal comparison.

Ground Truth Data

Ground truth values of sand coverage for each image were established by manually tracing the outline of sandy patches in each image. This work was done with a graphic user interface programmed in the MATLAB environment which allowed a user to trace the contours of sandy patches with the mouse and save the results. Ground truth values were then compared to detected values obtained by the automated routine.

Results

Initial results showed that in images with 0 per cent sand, automated texture segmentation falsely identified clast boundary areas as small slivers of sand. This can be explained by the contact of lighter clasts with darker voidspaces. The light/dark contact causes high textures which are then segmented into sand areas. Therefore, it was decided to implement a semi-automated phase in the process where a human user determines if sand is present or not. As a consequence, the six sub-images that were free of sand will not be considered in the analysis that follows since a human user quantified their sand presence to be 0 per cent.

In images where sand was present, the comparison of automatically detected versus ground truth sand coverage data was excellent. The relationship is $y = 1{\cdot}01x - 0{\cdot}96$ per cent with an R^2 value of 0·93 (Figure 3A). For each data point, the error was obtained by subtracting the predicted value from the ground truth value. The mean error for all points was 0·55 per cent which is interpreted as the overall accuracy (bias) for the method. The standard deviation was 4 per cent which can be interpreted as a precision of ±4 per cent.

In comparison, standard grey-level segmentation performed very poorly. The regression equation was $y = 0{\cdot}47x + 24{\cdot}35$ per cent with an R^2 value of 0·53 (Figure 3B). The bias was 1·4 per cent and the precision ±14 per cent.

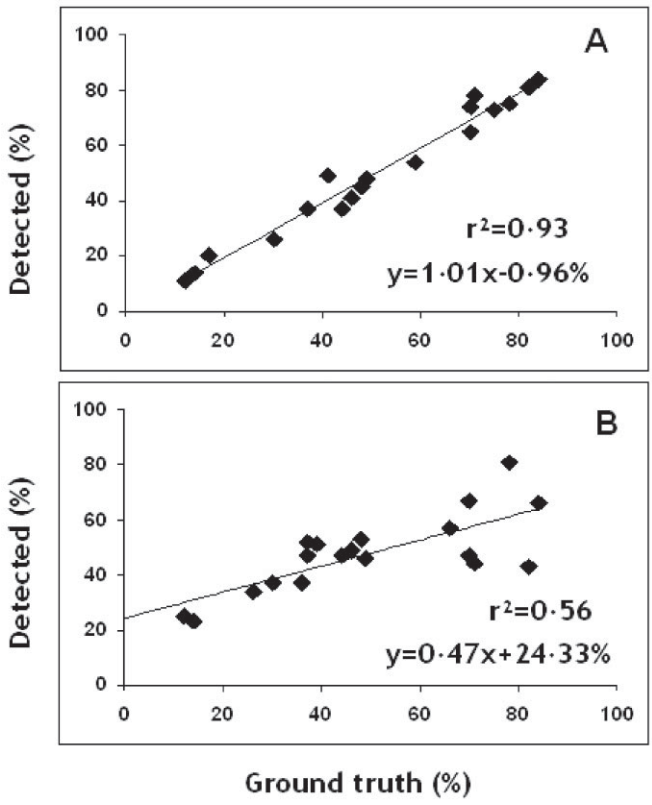

Figure 3. Validation relationships for sand quantification procedures. (A) Texture-based procedure. (B) Standard grey-level procedure.

Discussion

The 24·35 per cent offset and the 0·47 slope in the regression combined with the ±14 per cent precision for the standard grey-level segmentation method demonstrate the poor performance of the direct application of segmentation to the raw images. The high offset and the low slope indicate that in cases where sand coverage was low, the high background noise caused by individual sand grains with high brightness levels caused an important over-estimation of sand coverage. This over-estimation effect was proportionally higher in the low values, which in turn contributed to reducing the slope value. However, the results of the texture-based method are very encouraging. The slope of the regression is close to 1:1 and the offset is only 0·96 per cent. Additionally, the precision is estimated at ±4 per cent. These results indicate that the automated texture-based sand quantification procedure is reliable, accurate and precise.

Unfortunately, this method does have limitations. First, these results were obtained from images of dry exposed gravels. If applied to images of submerged gravels, the presence of water will predictably degrade the quality of results proportionally with the water's turbidity. Second, the method works best with coarse sand. It was observed that silts and clay have a very uniform appearance and therefore texture-based segmentation fails to highlight such areas. Finally, since the method works from imagery, it is limited to surface sand which is visible. However, despite the limitations this method does fill the need for a rapid assessment method of superficial sand. In this particular case, the images were collected from a gantry-mounted 35 mm film SLR camera. However, recent commercial digital cameras with megapixel resolutions can yield suitable imagery when hand-held over the target study site. If combined with a GPS survey, it is therefore possible to obtain hundreds of georeferenced image samples in a single day. Processing times for sand quantification are 3 min per image with a 1 GHz processor. Therefore in a 12 hour overnight batch process, 240 images can be analysed. The next step in this work is to test and adapt the procedure for images of submerged gravels. Such technology could allow for extensive sampling of superficial sand presence which could contribute valuable quantitative data to river-scale habitat quality quantification.

Conclusion

This paper shows that conventional grey-level segmentation is not applicable to the quantification of superficial sand presence in river gravels. The paper presents an alternative method capable of rapid and accurate assessments of superficial sand presence on fluvial gravels with a precision of ±4 per cent. The method is easy to deploy and requires only commercially available inexpensive technology and software.

Acknowledgements

The authors would to acknowledge funding from the GEOSALAR project and the GEOIDE network of centers of excellence. This work received additional funding from the NATEQ Ph.D. scholarship program. This is a contribution to the program of the Centre Interuniversitaire de Recherche sur le saumon atlantique (CIRSA).

References

Bunte K, Abt SR. 2001. *Sampling Surface and Subsurface Particle-Size Distributions in Wadable Gravel-and Cobble-Bed Streams for Analyses in Sediment Transport, Hydraulics, and Streambed Monitoring*. US Department of Agriculture, General Technical Report RMRS-GTR-74.

Castleman KR. 1996. *Digital Image Processing*. Prentice Hall: Upper Saddle River, NJ.

Chapman DW. 1988. Critical review of variables used to define effects of fines in redds of large salmonids. *Transactions of the American Fisheries Society* **177**(1): 1–21.

Church MA, Mclean DG, Wolcott JF. 1987. Bed gravels: sampling and analysis. In *Sediment Transport in Gravel-bed Rivers*, Thorne CR, Bathurst JC, Hey RD (eds). John Wiley: Chichester; 43–88.

Conners RW, Trivedi MM, Harlow CA. 1984. Segmentation of a high resolution urban scene using texture operators. *Computer Vision, Graphics and Image Processing* **25**: 273–310.

Cunjak RA, Prowse TD, Parrish DL. 1998. Atlantic salmon (*Salmo salar*) in winter: 'the season of parr discontent'?. *Canadian Journal of Fisheries and Aquatic Sciences* **55**(suppl. 1): 161–180.

Hall JD, Baker CO. 1982. *Influence of forest and rangeland management on anadromous fish habitat in western north America*. US Forest Service, General Technical Report PNW-138.

Haralick RM, Shapiro LG. 1985. Image segmentation techniques. *Computer Vision, Graphics and Image Processing* **29**: 100–132.

Haralick RM, Shanmugan K, Dinstein I. 1973. Textural features for image classification. *IEEE Transactions on Systems, Man and Cybernetics* **3**(6): 610–621.

IEEE. 1990. *IEEE Standard Glossary on Image Processing and Pattern Recognition Terminology*. IEEE Standard 610.4. IEEE Press: New York.

Otsu N. 1979. A threshold selection method from gray-level histograms. *IEEE Transactions on Systems, Man, and Cybernetics* **9**(1): 62–66.

Sear DA. 1993. Fine sediment infiltration into gravel spawning beds within a regulated river experiencing floods: ecological implications for salmonids. *Regulated Rivers* **8**: 373–390.

Soulsby C, Malcolm I, Youngson A. 2001. The hydrochemistry of the hyporheic zone in salmon spawning gravels: a preliminary assessment in a small regulated stream. *Regulated Rivers* **17**: 651–665.

Wentworth CK. 1922. A scale of grade and class terms for clastic sediments. *Journal of Geology* **30**: 377–392.

Wu FC. 2000. Modelling embryo survival affected by sediment deposition into salmonid spawning gravels:application to flushing flow prescriptions. *Water Resources Research* **36**(6): 1595–1603.

